Validation of the GSMaP Gauge NRT

*Tomoaki Mega[1], Tomoo Ushio[1]

1.Graduate School of Engineering, Osaka University

Information of real time precipitation is important for water disaster management. However real-time observation does not cover the whole world. Satellite observes global precipitation, although a satellite observation is limited overpass time. Global Satellite Mapping of Precipitation (GSMaP) is hourly rainfall map using combined passive microwave and infrared radiometric data from multi satellite. GSMaP in near-real-time (NRT) is providing data 4-hour after observation. Precipitation retrieval from the passive microwave radiometer underestimate over land. Gauge adjusted GSMaP (GSMaP Gauge) achived to compensate GSMaP MVK precipitation by gauge data. The method is not applied to GSMaP NRT, because we do not get global rain gauge data in 4 hour. We developed new GSMaP Gauge adjusted GSMaP NRT (GSMaP Gauge NRT). The new method estimate adjustment parameters for GSMaP NRT using previous GSMaP Gauge and GSMaP MVK. The method modify precipitation of the GSMaP NRT with these parameters. Distribution of monthly precipitation of GSMaP Gauge NRT is close to that of GSMaP Gauge. We will introduce GSMaP Gauge NRT algorithm and present validation of the GSMaP Gauge NRT.

Keywords: precipitation, microwave radiometer, GSMaP

Evaluation of the rain rate estimates of GPM/DPR using ground radar data

*Tatsuya Shimozuma[1], Shinta Seto[1]

1.Nagasaki University

1. Introduction

GPM (Global Precipitation Measurement) Core Observatory satellite has been in operation since February, 2014. GPM Core Observatory satellite is equipped with the Dual-frequency Precipitation Radar (DPR), the DPR consists of a Ku-band precipitation radar (KuPR) and a Ka-band precipitation radar (KaPR). The observation made with the spaceborne radar DPR is the first trial, and the evaluation is needed for the observation results. In this study, we focus on matchup cases with the XRAIN ground radar, and compare the rain rate estimates by DPR and XRAIN. Moreover, we discuss the reason of difference in the rain rate estimates.

2. Method

The Ministry of Land, Infrastructure, Transport and Tourism (MLIT) built the rainfall observation radar network called XRAIN. High frequency (every 1 minute) and high resolution (250m mesh) measurement becomes possible in comparison with a conditional ground radar. And XRAIN is operated at 39 places in Japan as of February 2016. And XRAIN is operated at 14 places in Japan as of February 2016. In this study, we focus XAIN radars to be operated in northern Kyushu region. Observation resolution is not same between DPR and XRAIN. The average is calculated from the XRAIN's rain rate included in DPR's footprint, and the rain rate estimates by DPR and XRAIN are compared. We used the DPR's rain rates at the clutter free bottom, which is stored as the variable name of [precipRateNearSurface]. The product version of DPR is V03B.

3. Comparison of the rain rate estimates between DPR and XRAIN

The rain rate estimates are compared between DPR and XRAIN. As DPR and XRAIN make different observation area, their match-up data that satisfy the following conditions, (1) the observation area is overlap, (2) some degree of rain rate is observed, were extracted. 50 matchup cases of DPR and XRAIN are found between June 2014 and January 2016. In this section, a match-up data at 03:27 (JST) of July 7th, 2015 (DPR orbit number:7703) is presented. The rain rate estimates of DPR and XRAIN are shown in Fig.1. The rain rate estimates of XRAIN are overestimated, and the area where rain is detected are different. The linear distribution are found in XRAIN's rain rate. The scatterplot of the rain rate between XRAIN and DPR is shown in Fig.2. X-axis is XRAIN's rain rate, and Y-axis is DPR's rain rate. Red symbols are for stratiform rain and blue symbols are for convective rain. From Fig.2, observation data that surrounded by XRAIN side show that XRAIN's estimates are higher than DPR's estimates. And the bias is negative value.

4. Comparison of the rain rate estimates in 50 matchup cases between DPR and XRAIN

In this section, the rain rate estimates of 50 matchup cases are evaluated. 2-D histogram of the rain rates between XRAIN and DPR is shown in Fig.3. Red line shows DPR's average rain rate estimates for XRAIN. From the Fig.3, the rain rate estimates of XRAIN are overestimated. And the average line is high in XRAIN rain rate over 0.6mm/hr. The factors of the differences are (1) measurement height is not same and (2) the estimation accuracy decrease as far from the central point of the radar. As DPR can provide the 3-dimensional rain rate distribution, in the future, we will compare the rain rate estimates at the same height.

5. Conclusion

GPM Core Observatory satellite has been in operation since February 2014. The observation made with DPR is the first trial, and the evaluation is needed for the observation results. We focus on the observation result of the XRAIN, and compare the rain rate estimates by DPR and XRAIN. As a result

of comparison, the rain rate estimates of XRAIN are overestimated. The factors of the differences are focus height and distance from the ground radar. In the future, we will compare the rain rate estimates at the same height.

Keywords: Global Precipitation Measurement (GPM), Dual-Frequency Precipitation Radar (DPR), MLIT X-Band MP Radar Network (XRAIN)

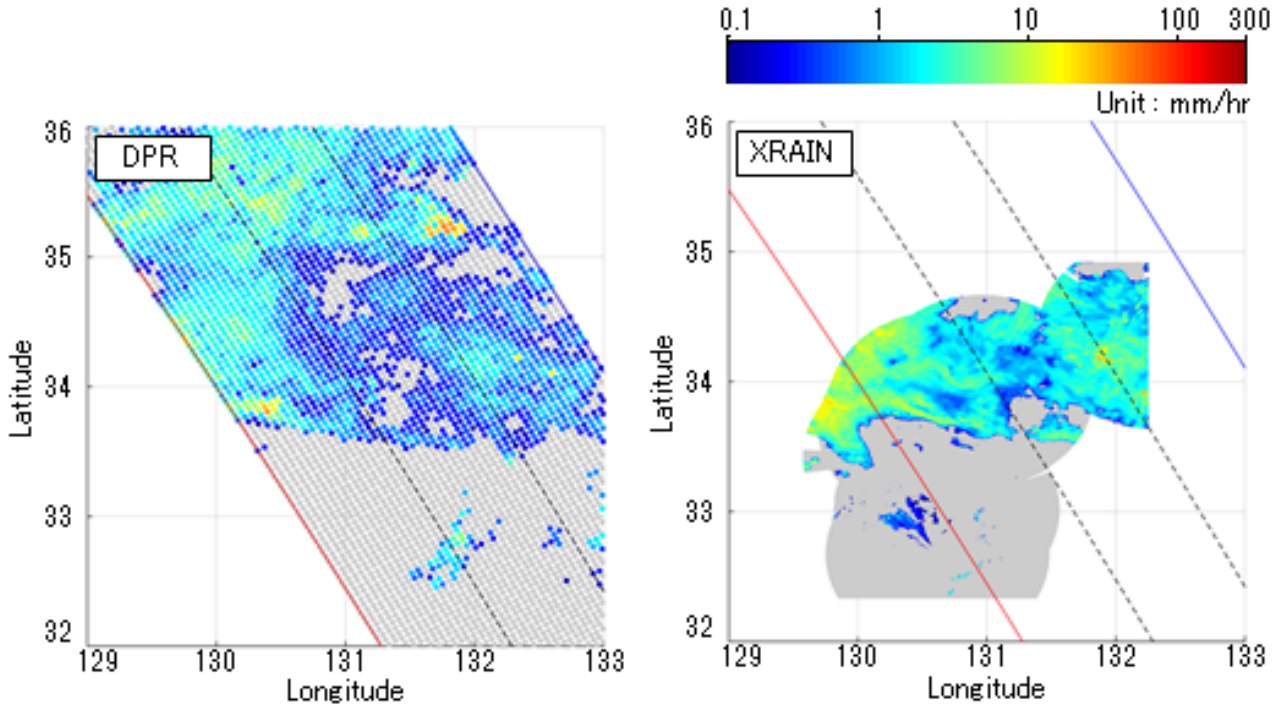

Fig.1 The rain rate estimates

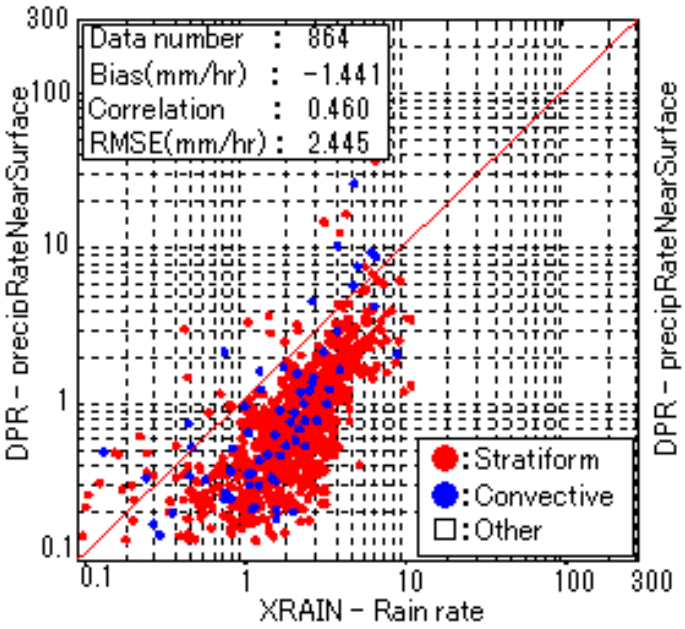

Fig.2 Scatterplot of the rain rate

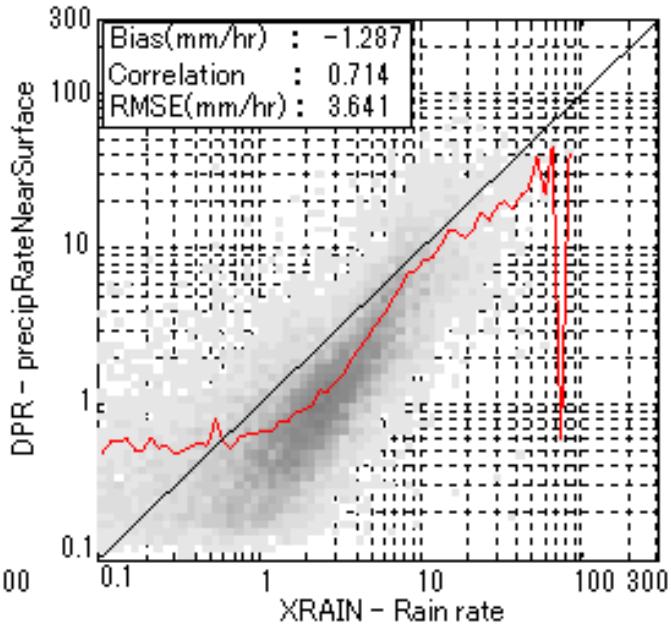

Fig.3 2-D histogram of the rain rate

A difference in the interannual variability of precipitation between PR and TMI

*Kaya Kanemaru[1], Takuji Kubota[1], Misako Kachi[1], Riko Oki[1], Toshio Iguchi[2], Yukari Takayabu[3]

1.earth observation research center, japan aerospace exploration agency, 2.National Institute of Information and Communications Technology, 3.Atmosphere and Ocean Research Institute, University of Tokyo

Precipitation has an important role in maintaining the hydrological cycle on the earth's climate, so that understanding the long-term variability of precipitation is essential to provide for the future such as the decadal climate variability or the climate change. It is, however, well known that the interannual variability of precipitation associated with El Nino Southern Oscillation (ENSO) is different between the Tropical Rainfall Measuring Mission (TRMM) Precipitation Radar (PR) and the TRMM Microwave Imager (TMI) estimates (Robertson et al. 2003; Wang et al. 2008; Lau and Wu 2011). The current study is aimed to explore the origin of the difference of the interannual variability of precipitation between PR and TMI.
The current study focuses on the differences in the precipitation type (convective and stratiform types) and its interannual variability. The precipitation estimates derived from PR (2A25; Iguchi et al. 2009) and TMI (2A12; Kummerow et al. 2011) products are individually divided into stratiform and convective precipitation estimates. The PR product contains results of the precipitation type in each pixel, but the TMI product contains together in same pixel. These data are projected onto a common 0.5 degrees gridded instantaneous data with ascending and descending orbits and sampled only where PR and TMI observations are available. Data are analyzed in the El Nino season (December 1997 to May 19998) and the La Nina season (December 1999 to May 2000) and compared between PR and TMI. Differences in unconditional precipitation average of convective and stratiform types over semi-global (35S-35N) oceans are overall same between PR and TMI in the La Nina season, because the database for the TMI retrieval was generated by means of the PR observation in this period. On the other hand, the difference in the convective precipitation between PR and TMI (TMI is generally higher than PR) are obviously found in the El Nino season, while the stratiform precipitation is similar between PR and TMI. The regions where the difference in convective precipitation between PR and TMI are large are found in warm sea surface temperatures (SSTs) for 300 to 303 K and moist column water vapors (CWVs) for 66 to 75 mm and frequently located over the central Pacific in the El Nino season. In the El Nino event, the ratio of stratiform precipitation against total precipitation central Pacific was increased (Schumacher and Houze 2003), which implies that the TMI does not follows the interannual nature-variability of the precipitation characteristics observed by the PR.

Keywords: Precipitation Radar, Microwave radiometer, Interannual variability

Additional information of precipitating cloud life stages for Improvement of rain rate data estimated from Himawari-8

*Hitoshi Hirose[1], Atsushi Higuchi[1], Tomoaki Mega[2], Tomoo Ushio[2], Munehisa K Yamamoto[3], Shoichi Shige[3], Atsushi Hamada[4]

1.Center for Environmental Remote Sensing, Chiba University, 2.Department of Engineering, Osaka University, 3.Department of Science, Kyoto University, 4.Atmosphere and Ocean Research Institute, The University of Tokyo

Rain observation with microwave radiometer satellites is essential to make global rain observation data with high temporal resolution. However microwave satellites cannot cover a global area since the number of them is limited. In such an area where no microwave satellite is available, improvement of rain estimation accuracy is expected by using rain information obtained from geostationary meteorological satellites (GMS) with high temporal resolution. Kühnlein et al. (2014) reported that they could estimate rain with high temporal resolution same as GMS by using a statistical method called Random Forest (RF) , which 10 channels information of brightness temperature observed from METEOSAT Second Generation (MSG-2) GMS are associated to truth of rain observed from ground-based radar. In this method, first some channels are selected from among GMS observations to make a classification tree deciding rain or no rain areas. Then the number of tree is increased in the same way, and finally rain or no rain area is decided by majority of all tree's results. In addition rain type classification and rain rate estimation are possible by the RF method. This study produced a new rain estimation product with high temporal resolution by applying this RF method to the only third generation GMS, Himawari-8 for compensating the lack of microwave satellites observation network. Moreover we used the Global Precipitation Measurement (GPM) main satellite instead of ground-based radar for the truth of rain used in machine learning for expanding the analysis area to all of the Himawari-8 observing area.
For verification of the above product, the threat score of the rain area estimated from Himawari-8 was calculated by comparing with rain observed by ground-based radar in near Japan region as the truth. As a result, the threat score in daytime is very high value more than 0.5, and that in night time is more than 0.42, which are conditionally comparable to microwave rain estimation. Next we verified effectiveness of Himawari-8 new additional channels to rain estimation. Then in rain area classification, a visible blue channel (0.46μm) is most effective and in rain type classification a near Infrared channel (1.6μm) is most effective. Route mean square error of rain rate is about 1.3 mm par hour but strong rain greater than 8.0 mm par hour is tend to be underestimated. This is partly because that it is difficult to distinguish thick convective cloud from thin cirrus since the rain rate estimated by RF method is mainly based on cloud top temperature (height) information obtained from Himawari-8 observation of brightness temperature. To overcome this problem, we tried to improve an accuracy of estimating convective rain rate by using temporal variation information of rainy cloud. First a moving vector of rainy cloud is calculated from every 10 minutes global observation of Himawari-8. Next we added temporal variation information of rainy cloud brightness temperature obtained by tracing rainy cloud with the moving vector into the RF method. As a result the Himwari-8 rain rate product is improved with life stage information of rainy cloud. We intend to show example analysis of the improved Himawari-8 rain product in near Japan region.
Himawari-8 GMS data is released from the Center for Environmental Remote Sensing, Chiba University. We used near surface rain observed by GPM (Ku PR) and rain intensity observed by ground-based radar in the Japan Meteorological Agency as the truth of Rain

Keywords: Himawari-8, GPM, precipitation, GSMaP

Climatological Cloud Database Estimated by Geostationary Satellite Split-Window Measurements

*Noriyuki Nishi[1], Atsushi Hamada[2], Hitoshi Hirose[3], Hitoshi Mukougawa[4]

1.Faculty of Science, Fukuoka Universtiy, 2.AORI, University of Tokyo, 3.CEReS, Chiba University, 4.Disaster Prevention Research Institute, Kyoto University

We extended our cloud-top database spatially to the midlatitude and temporally to new satellite Himawari-8. We have already released a database of cloud top height and visible optical thickness (CTOP) with one-hour resolution over the tropical western Pacific and Maritime Continent, using infrared split-window data of the geostationary satellites (MTSAT-1R and MTSAT2) (http://database.rish.kyoto-u.ac.jp/arch/ctop/). By comparing MT-SAT IR observation and the direct observation of the cloud top height by CloudSat radar, we can construct a lookup table (LUT) with which the cloud top height is estimated by using only MTSAT data. Unfortunately, now in the age of Himawari-8 that has been available since July 2015, the CloudSat observations are limited in the daytime and the precise direct comparison with the data cannot be conducted to construct LUT. Therefore, we proceeded an alternative way by constructing a calibration table based on the comparison between MTSAT-2 and Himawari-8 observations during July 2015 when both geostationary satellites were in operation. By using the similar approach repeatedly, it will be possible to construct LUT for the past geostationary satellites that had been in operation before the launch of CloudSat in 2006.
We also tried to extend the targeted region to the mid-latitude. In our present scheme applicable for only tropics, the vertical profile of temperature is assumed to be almost constant in whole tropics and all the year. However, since the temperature variability is much larger in mid latitude, it is not plausible to assume that the same IR radiance comes from the clouds with a certain top height. Therefore, we proposed a new method to use temperature data of the global analysis together. The temperature of the cloud top is estimated through the altitude of the cloud top observed by CloudSat as well as the temperature profile deduced from the global analysis data. Then we constructed LUT of cloud top temperature (not height) by the regression of the MTSAT IR radiance with respect to cloud top temperature. We can get the cloud top height at any point at any time by converting the cloud top temperature to cloud top height, with using global analysis data. A preliminary estimate using this method indicated that the cloud top height is estimated within allowable error even in the mid latitude.

Keywords: geostationary satellite, cloud, database

Simultaneous retrieval of aerosol optical thickness and chlorophyll concentration using multi-wavelength and multi-pixel method

*CHONG SHI[1], Teruyuki Nakajima[1], Makiko Hashimoto[1], Hideaki Takenaka[1]

1.JAXA/EORC

This study proposes an algorithm for the simultaneous retrieval of aerosol optical thickness(AOT) and chlorophyll concentration using multi-wavelength and multi-pixel method over ocean. In our algorithm, the forward radiation calculation is performed by a coupled atmosphere-ocean model(Ota et al., 2010; Nakajima and Tanaka, 1986) with an improved bio-optical ocean module(Shi et al., 2015) for CASE 1 water, which is different to the traditional ocean color algorithms which decouple the atmosphere and ocean surface(Gordon and Wang, 1994) using atmospheric correction procedures; then the Maximum a posterior method(Rodger, 2000) but considering the spatial constrain incorporated with the multi-pixel optimization algorithm(Hashimoto, 2014) is used to retrieval aerosol optical thickness and chlorophyll concentration. For the AOT retrieval, a global aerosol transport-radiation model named SPRINTARS(Takemura et al,. 2000) is used as the priori constrain; Finally, the inversion results are achieved from HIMAWARI-8 and GOSAT-TCAI satellite observation data through comparison to AERONET products and other aerosol retrieval algorithm which is widely used in satellite remote sensing.

Keywords: Aerosol, Ocean color, Remote sensing, Radiative transfer

Simultaneous observations of solar-induced chlorophyll fluorescence by vegetation and atmospheric CO_2 dynamics by GOSAT

*Hibiki M Noda[1], Kouki Hikosaka[2], Kazutaka Murakami[1], Tsuneo Matsunaga[1]

1.NIES National Institute of Environmental Studies, 2.Tohoku University

In these decades, global warming has progressed owing to increase of greenhouse gases (GHGs) such as CO_2. To deal effectively with this issue by mitigation and adaptation, it is necessary to monitor emission and sequestration of GHGs with their underlying mechanisms including biogeochemical processes and human activities. Terrestrial ecosystem, which is the large carbon sink, absorbs 123 Pg carbon per year through plant photosynthesis (IPCC 2014). Satellite remote sensing has been used to monitor the spatial and temporal dynamics of terrestrial ecosystems that are responsible for such photosynthetic CO2 absorption. Such observation provides us with geographical information on the potential distribution of carbon sequestration by the aid of ecosystem models. However, as the photosynthesis of a given vegetation is quite sensitive to meteorological changes such as radiation, temperature and precipitation, we need to observe the photosynthetic ‘activity’ in a physiological sense, together with the atmospheric CO2 concentration over continental and global scales. Joiner et al. (2011) and Frankenberg et al. (2011) have suggested that TANSO FTS on Greenhouse Gases Observing Satellite (GOSAT) could detect overlapping part of solar-induced chlorophyll fluorescence (SIF) emitted by terrestrial vegetation and Fraunhofer line. The chlorophyll fluorescence is photons of red and far-red light that emitted by chlorophylls, and in plant ecophysiology it has been a biophysical index to examine the photosynthetic responses to environmental stresses such as extreme temperatures and drought. Thus SIF remote sensing is drawn considerable attention as a new technique to observe the photosynthetic activity of the vegetation. This paper will present our on-going and future challenges by GOSAT and GOSAT-2 to observe such photosynthetic activity of terrestrial ecosystems and its possible consequences with the atmospheric CO2 concentration from national, continental to global scales under climate change.

Keywords: carbon cycle of terrestrial ecosystem, photosynthetic production

Preliminary sensitivity study of the GOSAT-2 FTS SWIR retrievals based on the designed specifications

*Yukio Yoshida[1], Akihide Kamei[1], Isamu Morino[1], Makoto Saito[1], Hibiki Noda[1], Tsuneo Matsunaga[1]

1.NIES

The Greenhouse gases Observing SATellite (GOSAT) was launched in January 2009 and observed global distribution of the column-averaged dry air mole fractions of carbon dioxide and methane (XCO_2 and XCH_4) for about seven years. As a successor mission to the GOSAT, GOSAT-2 is planned to be launched in early 2018, and its critical design review (CDR) was completed. GOSAT-2 also has a Fourier transform spectrometer (FTS) like GOSAT to obtain short-wavelength infrared (SWIR) light reflected from the earth's surface and thermal infrared (TIR) radiation emitted from the ground and atmosphere. According to the current design of the FTS-2 (FTS onboard the GOSAT-2), its SNR is higher than or almost equal to that onboard the GOSAT, and it covers the 2.3 μm carbon monoxide (CO) band as well as the 1.6 and 2.0 μm CO_2 bands and 1.67 μm CH_4 band. Our preliminary sensitivity test shows that the SNR improvement in SWIR bands reduces the retrieval random error (precision) about 15% for XCO_2 and 35% for XCH_4 than those of GOSAT.

Keywords: GOSAT-2, XCO2, XCH4

Applied FORMOSAT-3/COSMIC on observing atmospheric temperature changes caused by volcanic eruptions

*Chun-Chieh Hsiao[1], Jann-Yenq Liu[2], Hsin I Lai[1], Yi Cheng Chiu, Shiann-Jeng Yu[1], Guey-Shin Chang[1]

1.National Space Organization, 2.Graduate Institute of Space Science, National Central University

Volcanic eruptions are often along with fiery magma, hot dense gases and powerful explosive energy. Those materials injected into atmosphere might cool tropospheric temperature and warm the temperature of bottom of stratosphere but sometimes the phenomenon was exactly opposite or mixture. This study focused on 8 volcanic eruptions, the explosive indexes of which were 4 during 2008 to 2011 and analyzed the temperature-related data from radio occultation observations of FORMOSAT-3/COSMIC (F3/C). It individually investigated the temporal latitude-altitude and longitude-altitude variances atmospheric temperatures from northeastern, northwestern, southeastern and southwestern of volcanos before and after the eruptions. This study also observed the image from Moderate resolution Imaging Spectroradiometer (MODIS) on NASA terra satellite to see where the volcanic plum extended. Results apparently show that 3 events had cooling troposphere and warming bottom of stratosphere and 2 events were just the opposite. One of the rest events was mixture case and the other one of the rest was without apparent variances in temperature. Cooling troposphere and warming bottom of stratosphere caused by stratospheric aerosols that reduced sunlight reaching troposphere and absorbed radiation at the bottom of stratosphere. The consequence opposite to above was caused by that volcanos erupted hot and high density gases into troposphere and adiabatic expansion happened during the top of troposphere and bottom of stratosphere. Moreover, in mixture case, area with more volcanic ash showed decreasing temperature in the troposphere and increasing temperature at the bottom of stratosphere. Area with less volcanic ash showed increasing temperature in the troposphere and decreasing temperature at the bottom of stratosphere.

Keywords: FORMOSAT-3/COSMIC, volcano

Cloud properties analysis based on EarthCARE/MSI observation

*Seiko Takagi[1], Takashi Nagao[2], Haruma Ishida[3], Husi Letu[4], Makiko Hashimoto[2], Takashi Nakajima[5]

1.Tokai University, Research and Information Center, 2.Japan Aerospace Exploration Agency, 3.Meteorological Research Institute, 4.Institute of Remote Sensing and Digital Earth, Chinese Academy of Sciences (CAS), 5.Tokai University, School of Information Science & Technology, Dept. of Human & Information Science

Clouds and aerosols are the major uncertainty in the understanding of the Earth’s climate system. An improvement of understanding and better modeling of the relationship of clouds, aerosols and radiation are therefore prominent part in climate research and weather prediction. It is important to obtain the global data of clouds and aerosols occurrence, structure and physical properties that are derived from measurements of solar and thermal radiation.
EarthCARE (Earth Clouds, Aerosols and Radiation Explorer) is one of the future earth observation mission of ESA and JAXA. The satellite will carry four instruments for observation of clouds and aerosols; Atmospheric Lidar (ATLID), Cloud Profiling Rader (CPR), Multi-Spectral Imager (MSI), and Broad-Band Radiometer (BBR). This mission aims at understanding of the role that clouds and aerosols play in reflecting incident solar radiation back into space and trapping infrared radiation emitted from Earth’s surface. These observations are needed to improve the precision of climate variability prediction.
MSI provides across-track information on cloud with channels in the visible, near infrared, shortwave and thermal infrared. Water cloud optical properties are derived in using EarthCARE/MSI standard product based on CLAUDIA [Ishida and Nakajima, 2009] and CAPCOM [Nakajima and Nakajima, 1995; Kawamoto et al., 2001]. Research product based on MWP method [M. Hashimoto, 2015. PhD Thesis] is advanced to obtain the ice cloud optical properties. In this presentation, development of the cloud analysis algorithms will be introduced.

Keywords: EarthCARE, cloud

Development of remote sensing algorithm to retrieve aerosol optical properties and introduction of the results of case studies

*Makiko Hashimoto[1], Hideaki Takenaka[1], Akiko Higurashi[2], Teruyuki Nakajima[1]

1.Japan Aerospace Explortion Agency, 2.NIES

We have developed a satellite remote sensing algorithm to retrieve the aerosol optical properties using multi-wavelength and multi-pixel information of satellite imagers (MWP). We simultaneously retrieve several parameters that characterize pixels, such as aerosol optical thickness (AOT) of fine and coarse mode particles, single scattering albedo (SSA), and ground surface albedo of each observed wavelength, in each of horizontal sub-domains consisting the target area.
We applied the algorithm to GOSAT/TANSO-CAI and Himawari-8/AHI data. We will show the retrieval results of aerosol characteristics over the urban and forest fire regions such as the Kanto area in Japan and Beijing in China. We also tried to retrieve aerosol properties at a forest fire case, so we would like to introduce the retrieval results over the forest fire regions in Indonesia.
From the results, AOT over the urban or high population areas is larger than that around rural or the low population areas. Furthermore, the SSA is lower in the urban region. For the forest fire case, the AOT and SSA along the plume are higher and lower than that of the other region, respectively. Although the AOT of fine mode totally looks dominant, the Angstrom exponent around the hot spot is lower than that of the leeward side, and increase with the increasing distance from the hot spot.

Keywords: Remote sensing, Aerosol, Satellite

Eddy Effect on the Kuroshio East of Taiwan from Satellite Altimetry

*Chungru Ho[1], Po-Chun Hsu[1], Chen-Chih Lin[1], Shih-Jen Huang[1]

1.Natl. Taiwan Ocean Univ.

Kuroshio is a western boundary current in the North Pacific Ocean. It flows northward along the east coast of Taiwan. Previous studies have shown that there is an eddy-rich zone located at 18°-26°N, 122°-160°E. The westward propagating eddies may affect the axis of Kuroshio when they impinge the Kuroshio east of Taiwan. To more understand the phenomenon, satellite altimeter data are used to investigate effects of oceanic mesoscale eddy on the Kuroshio from 18°N to 26°N. The Kuroshio axis is defined as a line with the maximum surface velocity along the Kuroshio path. The velocity of Kuroshio is calculated from the absolute dynamic topography data derived from satellite altimetry with the geostrophic relations. The results show that the Kuroshio meander occurred 13 times from 1993 to 2013 which were caused by westward or northward moving cold eddies when they propagated to the east of Taiwan. The average duration of the meanderings was 27 ±20 days, and the maximum duration was 80 days. The farthest position of the Kuroshio axis meandering was approximately 270 km from the average Kuroshio axis. It is affected by the size of the cold eddy. Under the circumstances of a cold eddy, the mean speed of the Kuroshio axis drops to 0.63 m/s, which is approximately 84% of the seasonal average.

Keywords: Kuroshio, meander, eddy, satellite altimetry

The Central-Pacific type of ENSO and its connection to Pacific Meridional Mode

*ChunYi Lin[1]

1.National Museum of Marine Science & Technology

In this study, we examine the simulation of the Pacific meridional mode in pre-industrial experiments of the Coupled Model Intercomparison Projects Phase (CMIP5) and link the Pacific meridional mode simulations to the simulation of the Central-Pacific (CP) and Eastern-Pacific (EP) types of El Niño Southern Oscillation (ENSO). Objective criteria are developed to evaluate the model performance in Pacific meridional mode simulations, which gauge the intensity, spatial pattern, air-sea coupling strength, and persistence strength of the coupling of the model meridional mode. Our analyses indicate that most of the CMIP5 model overestimate the air-sea coupling strength in the subtropical where the Pacific meridional mode model occurs, but underestimate the persistence of the coupling. Based on our criteria, ten CMIP5 models are found capable of realistically simulating the Pacific meridional mode. Further analyses reveal that CMIP5 model simulations of the CP ENSO is linked to the model performance in simulating the Pacific meridional mode; the models that are more capable of simulating the Pacific meridional mode also produce stronger CP ENSO. This study demonstrates that the subtropical dynamics and coupling affect the ability of CMIP5 models in simulating the different flavors of ENSO, which should be considered as one of the importance matrices for CMIP5 model evaluation.

Keywords: Central-Pacific types of ENSO, Eastern-Pacific types of ENSO, Pacific meridional mode

Validation of AMSR2 ocean products –Construction of validation system–

*Tsutomu Hihara[1], Hiroyuki Tomita[2]

1.Tokai University, Doctor's Course of Earth and Environmental Science, 2.Nagoya University, Institute for Space-Earth Environmental Research

In Global Change Observation Mission (GCOM), a satellite named GCOM-Water (GCOM-W) was launched in May 2012 to observe the effective geophysical parameters for understanding the global change of water cycle. The Japan Aerospace Exploration Agency (JAXA) has provided the ocean products (sea surface temperature and sea surface wind speed), which are made from brightness temperature observed by the Advanced Microwave Scanning Radiometer 2 (AMSR2) loaded onto GCOM-W, since May 2013. In general, satellite products are updated frequently, because the validation of data and the development of algorithm continue after these were released. The JAXA already updated the AMSR2 ocean products one time and will continue the updating. Accordingly, we tried to develop a validation system (VS) offering continuously and speedily the significant information for improvement of products in order to validate the AMSR2 ocean products from a long-term perspective and under a unified reference.

The VS mainly consists of two components. The first component is “Inter-comparison between the several gridded data”. In this component, the VS outputs the spatial distributions of average and standard deviation for each grid datum, the time series of the regional mean, and the mean difference and the Root Mean Square (RMS) difference between the grid data and the reference data that are made preparations in advance. The second component is “Comparison with in situ data”. In this component, the grid data are compared with high quality meteorological data observed by the moored buoys or the ships. As a result, the basic statistics (bias, RMS error, correlation coefficient and so on) and the figures (scatter plot and time series on buoy positions) are obtained. About the above-mentioned results, we can graphically check by the html files, which are automatically created in the VS.

As an example, we show the screenshots of results of comparison between AMSR2 sea surface temperature data and moored buoy data in an attached figure. In this result, AMSR2 data were validated using 24,660 daily mean data observed by 97 moored buoys from 2012 to 2014. We can check not only the results for all buoy data, but also the results for each year, each band of latitude, and each buoy.

Keywords: GCOM-W, AMSR2, mooring buoy data, marine meteorology, sea surface temperature

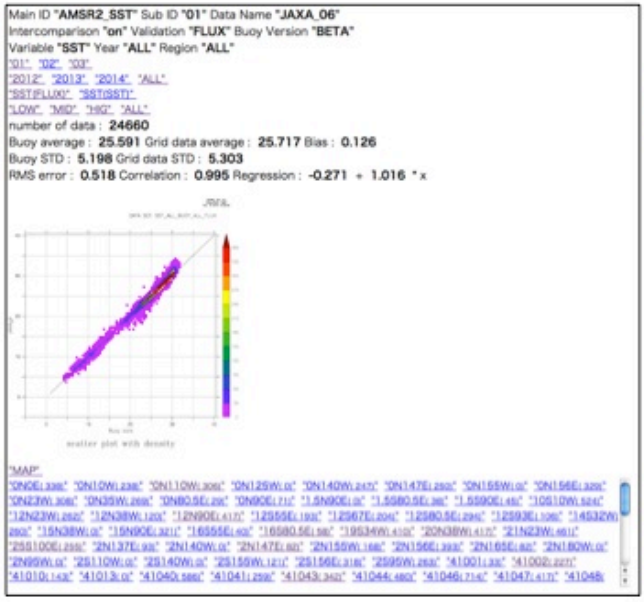

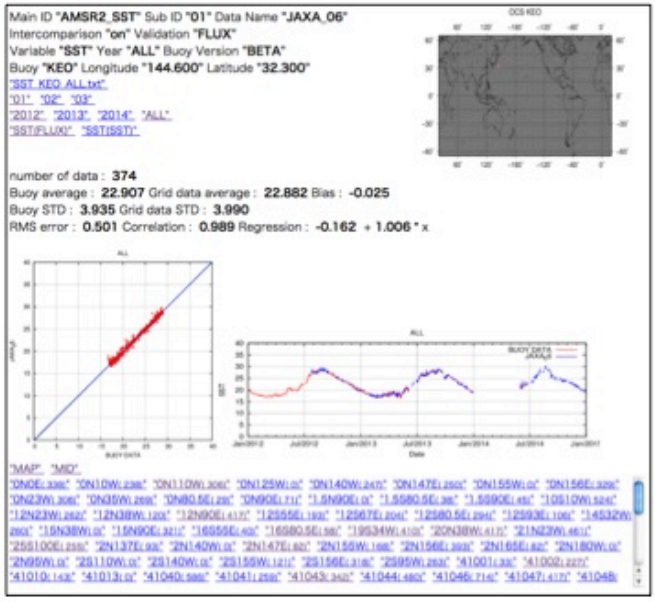

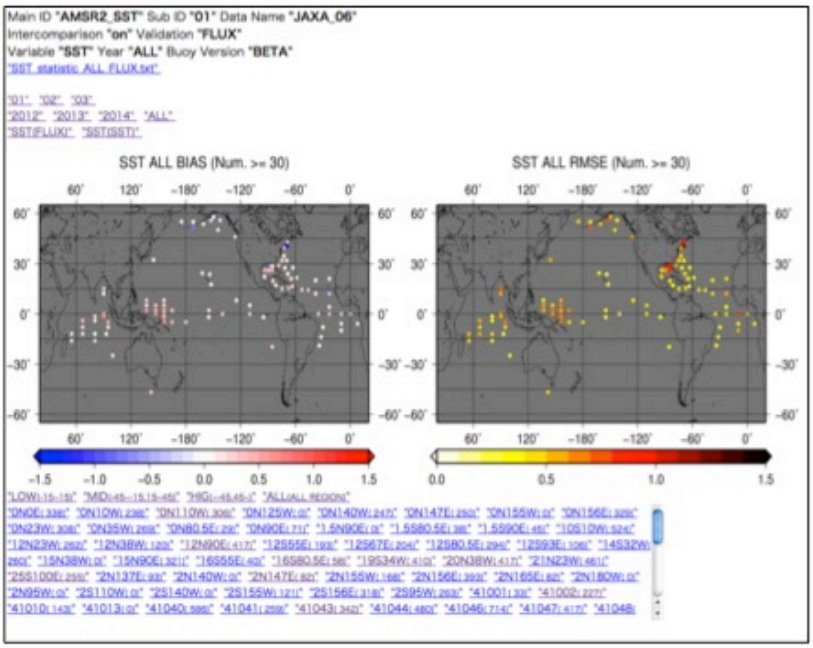

Applying Big Data Analysis Method to Improvement Sea Surface Temperature of Geostationary Satellite.

*Yung Shiang Lee[1], Feng Chun Su[2], Yu Mei Yeh[1], Chun Yi Lin[2], Yu Hsin Chen[3]

1.Department of Marketing & Distributioin Management, Hsiang Wu University, 2.National Museum of Marine Science & Technology , Taiwan, 3.State Key Laboratory of Marine Environmental Science, College of Ocean and Earth Sciences, Xiamen University, Xiamen, China

Big Data is the amount of data involved enormous and cannot be the information within a reasonable period of time to query, retrieve, manage, and analyze. The Big Data are three qualities: Volume, Velocity, and Variety, which information in many fields have brought progress and a breakthrough opportunity. Recent studies sea surface temperature mostly as a reference material Moderate Resolution Imaging Spectroradiometer (MODIS). Sun-synchronous satellites significantly better than geostationary satellites at a time resolution. The equatorial region of the tropical Pacific SST bias main factors are wind speed and air temperature in past studies. In this study, used big data commonly algorithms to provide sea surface temperature (SST) image hourly data. We apply and compare data mining techniques to improve the quality of GOES SST product. By a logistic regression approach, the GOES SST can be determined with an accuracy of 0.4°K and an improvement of the correction to 95%.

Keywords: Big Data, Sea Surface Temperature, Tropical Pacific

The Evolution of internal wave from mode-one to mode-two

*fengchun Su[1]

1.National Museum of Marine Science & Technology

Internal waves (IWs) are observed in the ocean all over the world. In the northern South China Sea, internal waves are frequently monitored between the Luzon Strait and Hainan Island by several satellites, such as optical or radar satellites. The wave crest can be as long as 200 km. It's amplitude is larger than 170 m. The huge amplitude maybe the largest than that ever observed in the world's oceans. The huge IW is usually observed in the deep sea area between the Luzon Strait and Hainan Island. Then a small mode-two wave was observed following a huge mode-one IW on the shelf near Dong-Sha Atoll. Due to the different wave speeds, mode-one and mode-two waves would separate into two waves after decomposition on the shelf. Thus we though the huge model-one IW in deep sea area could be deposited into more modes of IW on the shelf.
In this study, the objective is to observe the generation and evolution of mode-one IWs in the deep sea area, and then the mode-one IW deposit into more modes of IWs on the shelf break. The generation of mode-two waves on the shelf by disintegration of mode-one IWs in the deep ocean is proposed and analyzed based on the theory of modal-decomposition. In this study, some historical measurement data and satellite image are used to detect IWs. Then , the environmental condition is from a mooring near Dong-Sha Island. For comparison, the characteristics of mode-one and mode-two waves from environmental parameters have been estimated. For the test case, water depth increases to 450 m the mode-two wave energy is decreasing to 14%, while it is increasing to 25% when water depth decreases to 350 m. So, the mode-two waves can be generated under favorable condition, especially for multiple layer stratification in the shallow water on shelf.

Keywords: internal wave, south china sea, mode-two

